J. Biochem. 2019;0(0):1–10 doi:10.1093/jb/mvz046

JB THE JOURNAL OF BIOCHEMISTRY

Production and characterization of monoclonal antibodies against the DNA binding domain of the RE1-silencing transcription factor

Received February 27, 2019; accepted June 6, 2019; published online June 14, 2019

Karen Cortés-Sarabia[1], Yolanda Medina-Flores[2], Luz Del Carmen Alarcón-Romero[1], Olga Mata-Ruíz[2], Amalia Vences-Velázquez[1], Hugo Alberto Rodríguez-Ruíz[1], Jesús Valdés[3] and Carlos Ortuño-Pineda[1,*]

[1]Facultad de Ciencias Químico Biológicas, Universidad Autónoma de Guerrero, Av. Lázaro Cárdenas s/n, 39090 Chilpancingo, Guerrero; [2]Instituto de Diagnóstico y Referencia Epidemiológicos "Dr. Manuel Martínez Báez", Francisco de P. Miranda 177, Lomas de Plateros, 01480 Ciudad de México and [3]Departamento de Bioquímica, Centro de Investigación y Estudios Avanzados del Instituto Politécnico Nacional, Av. Instituto Politécnico Nacional, 2508, 07360 Ciudad de México, México

*Carlos Ortuño-Pineda, Facultad de Ciencias Químico Biológicas, Universidad Autónoma de Guerrero, Av. Lázaro Cárdenas s/n, 39090 Chilpancingo, Guerrero, México1. Tel: +52-5531543508, Fax: +52 (747) 4720-390, email: ortunoc@outlook.com

The use of monoclonal antibodies for the detection of cellular biomarkers during carcinogenesis provides new strategies for cancer diagnosis or prognosis in patients. Loss of the Restrictive Element 1-Silencing Transcription (REST) factor has been observed in previous molecular and immunological approaches in aggressive breast cancer, small cell lung cancer, liver carcinoma, and colo-rectal cancer; however, for clinic diagnosis, monoclonal antibodies for REST recognition are unavailable. The goal of this work was to design, produce and characterize monoclonal antibodies against the REST DNA binding damain (DBD) that would be suitable for immunoassays. We searched for conserved domains, and immunogenic and antigenic sites in the REST structure via *in silico* analysis. For mice immunization, we used a recombinant REST DBD purified by affinity chromatography, and then Hybridomas were generated by mouse spleen fusion with myeloma cells. Finally, for monoclonal antibody characterization, we performed enzyme-linked immunosorbent (ELISA), western blot, dot blot, immunocytochemistry (ICC) and immunoprecipitation assays. Results showed that the DBD is conserved in REST isoforms and contains immunogenic and antigenic sites. We generated three clones producing monoclonal antibodies against REST DBD, one of them specifically recognized native REST and was suitable for ICC in samples from patients.

Keywords: DNA binding domain; immunoassays; monoclonal antibodies; NRSF; REST.

Abbreviations: CC, cervical cancer; DAB, 3-3′--diaminobenzidine; DBD, DNA binding domain; DMEM, Dulbecco's modified Eagle's medium; ELISA, enzyme-linked immunosorbent assay; HGSIL, high-grade squamous intraepithelial lesion; HRP, horseradish peroxidase; ICC, immunocytochemistry; IEDB,Immune Epitope Database and Analysis Resource; LGSIL, low-grade squamous intraepithelial lesion; mAb, monoclonal antibody; MHC, major histocompatibility complex; NRSF, Neuron-Restrictive Silencer Factor; NSIL, non-squamous intraepithelial lesion; OD, optical density; PBS, phosphate buffered saline; REST, Repressor Element 1-Silencing Transcription; RE1, Repressor Element 1; RT, room temperature; SCLC, small cell lung cancer; SDS-PAGE, sodium dodecyl sulphate polyacrylamide gel electrophoresis.

The Repressor Element-1 Silencing Transcription (REST) factor, also named Neuron-Restrictive Silencer Factor (NRSF) silences gene expression by binding to the Repressor Element 1 (RE1) sequence located in the promoter region of its target genes (*1*). Human, mouse and *Xenopus* genomes harbour hundreds of REST transcriptional targets, mainly involved in neurotransmission, ion transport, motility, angiogenesis, apoptosis, cellular replication, and protein synthesis (*2*–*6*). At a structural level, REST is a 1,097 amino acids protein, containing two repressor domains in the N- and C-terminals, and a central DNA binding domain (DBD) with eight zinc fingers (*7*, *8*). Notably, REST isoforms, lacking a C-terminal, play a key role in neurogenesis, regulating neuronal differentiation and some events of synaptic plasticity events, such as axonal growth, vesicular transport and ionic conductance (*9*, *10*). As a result, the loss of REST and expression of several REST isoforms are related with diseases, including Down syndrome, Huntington's disease, Parkinson's, cardiomyopathy, and cancers (*11*–*13*). In cells, REST acts as a tumour suppressor gene in epithelial phenotypes, because its inhibition increases the oncogenic transformation (*14*, *15*), and as an oncogene due to its association with *Myc* (*12*, *16*).

Many types of tumours express abnormal REST levels, such as colon (*16*), small cell lung cancer (SCLC) (*17*), breast (*18*–*20*), prostate cancers (*21*), medulloblastoma (*22*), glioblastoma multiforme (*23*), cholangiocellular carcinoma (*24*) and uterine fibroids, a benign tumours of the uterus (*25*). Similarly, a robust analysis from our workgroup, which included 400 samples of cervical cytology samples and 76 cervical tissues samples of patients showed a significant reduction in

REST expression in high-grade squamous intraepithelial lesion (HGSIL) and cervical cancer (CC). However, a normal, nuclear expression was observed in low-grade squamous intraepithelial lesion (LGSIL) and non-squamous intraepithelial lesion (NSIL), suggesting an important role for REST as a diagnostic or prognostic biomarker (under review).

Despite the acummulating evidence, showing the role of REST in carcinogenesis and cancer progression there is not a serious strategy for the production of monoclonal antibodies against REST suitable for clinic diagnostics. Some REST antibodies with high specificity and sensitivity are commercially available; however, they cannot be used for clinical purposes because they do not recognize the REST isoforms associated with cancer. For this reason, the aim of this work was to design, produce and characterize monoclonal antibodies to evaluate the potential use of REST as a diagnostic or prognostic marker for cancer.

Materials and Methods

In silico *analysis*

Analysis of the REST gene, mRNA and protein isoforms was performed as previously described (*8*, *26*) using the following NCBI accession numbers U22314.1 (REST), JX896960.1 (REST-1), JX896971.1 (REST-4), AF228045 (REST-50), JX896958.1 (REST-62), JX896959.1 (REST-5Δ) as mold. For protein structure prediction, we used the Atlas of Genetics and Cytogenetics in Oncology and Haematology of REST available online (*7*).

To search for immunogenic and antigenic sites, we first downloaded the REST sequence with the access number NP_001180437.1 (https://www.ncbi.nlm.nih.gov/protein/NP_001180437.1) from the NCBI GenBank. For B cell epitopes prediction we used ABCpred (http://crdd.osdd.net/raghava/abcpred/) (*27*) and Bcepred (http://crdd.osdd.net/raghava/bcepred/) softwares (*28*), while we used the Predicted Antigenic Peptides software (http://imed.med.ucm.es/Tools/antigenic.pl) (*29*) for determination of antigenic sites. Finally, the prediction and analysis of B and T cell epitopes were performed in the Immune Epitope Database and Analysis Resource (IEDB) (http://www.iedb.org/) (*30*).

REST DBD and RE1 sequence 3D structure prediction

To obtain the 3D structure of REST DBD (DBD), the I-TASSER server (https://zhanglab.ccmb.med.umich.edu/I-TASSER/) was used, and the model with the highest C-score (confidence score to estimate the quality of the models predicted by I-TASSER) was selected. This score was calculated according to alignments importance in the sub-processing template and convergence parameters in the assembly of structures simulations (*31–33*). The quality of the model was evaluated with the ERRAT server (http://services.mbi.ucla.edu/ERRAT/) (verification of the structure and interaction analysis of the obtained protein) where a quality factor of >50% is acceptable (*34*), the quality factor for the REST DBD was 76.4%.

For the RE1 3D structure generation, we used a the consensus of 21 nucleotides 5′-TTC AGC ACC ACG GAC AGC GCC-3′, which was analysed in the 3DNA-Driven DNA Analysis and Rebuilding Tool server (3D-DART) (http://milou.science.uu.nl/services/3DDART/) (*35*, *36*).

REST DBD docking to RE1 sequence

The 3D structural docking of the RE1 sequence to the REST DBD was performed using the NPDock (Nucleic acid-Protein Dock) server (http://iimcb.genesilico.pl/NPDock/) (*37*).

Recombinant REST DBD purification

Escherichia coli BL21 (DE3) strain (New England BioLabs Cat # C2527I) transformed with pET28a-REST DBD construct (Unpublished data) was reseeded in Luria-Bertani medium with ampicillin to reach an optical density (OD) of 0.5 at 600 nm. Recombinant protein expression was induced with 0.1 mM of isopropyl-β-D-thiogalactopyranoside) and purified by affinity chromatography using Ni-NTA columns (Qiagen Cat # 30210), according to manufacturer's instructions. The recombinant REST DBD was quantified by spectrophotometry, stored at −20°C, and used for mice immunization.

Monoclonal antibody production

Hybridomas were generated by the previously described method (*38*). Six-week-old Balb/C mice were immunized weekly with 25 μg of recombinant REST DBD protein and TiterMax Gold adjuvant (Sigma-Aldrich Cat # T2684). On day 35, a selected mouse was immunized only with the antigen dissolved in phosphate buffered saline (PBS), and 3 days later, mouse spleen cells were fused with X63-Ag8.653 myeloma cells using polyethylene glycol 1,500 (PEG/DMSO solution HybriMax, Sigma-Aldrich Cat # P7181). Hybrids were selected in Dulbecco's modified Eagle's medium (DMEM) supplemented with hypoxanthine, aminopterin and thymidine (50× HAT Media Supplement HybriMax, Sigma-Aldrich Cat # H0262). Culture supernatant samples were monitored by indirect enzyme-linked immunosorbent (ELISA) using recombinant REST DBD as antigen. Hybridomas secreting monoclonal antibodies (mAb) were subcloned twice by limiting dilution and maintained in DMEM (Sigma-Aldrich Cat # D5796) with 10% fetal bovine serum (Gibco Cat # 16000044) and antibiotics. All procedures involving mice manipulation were performed in accordance with the bioethical regulations of the Instituto de Diagnóstico y Referencia Epidemiologica (InDRE) in Mexico City.

For quantitative analysis, mAbs were purified from the culture medium using HiTrap IgM columns (GE life sciences Cat # 17-5110-01) following manufacturer's instructions. Purified IgM (mg/mL) concentration was determined by measuring the OD at 280 nm divided by 1.18 (extinction coefficient of IgM).

Enzyme-linked immunosorbent assay (ELISA)

Immune response evaluation in the immunized mice, hybrids selection, mAbs immunoglobulin class, REST DBD recognition, antigens and mAbs concentration titration were determined by indirect ELISA. Microtiter plates (Sigma-Aldrich Cat # CLS3590) were coated with recombinant REST DBD by adding 100 μL of protein solution (10 μg/mL) in coating buffer (50 mM Na_2CO_3/$NaCO_3H$ pH 9.6) and incubated overnight at 4°C. Plates were blocked for 30 min at room temperature (RT) with 200 μL of 5% skimmed milk in PBS-Tween 0.05% and then incubated with serum, culture supernatant or purified mAb for 2 h at 37°C. After washing, plates were incubated with 100 μL (dilution 1:2,000) of anti-mouse H + L (Jackson ImmunoResearch Cat # 115-035-003), anti-Mu (Jackson ImmunoResearch Cat # 115-036-020) or anti-Gamma (Jackson ImmunoResearch Cat # 309-036-008) coupled to horseradish peroxidase (HRP), in PBS-Tween 0.05% and incubated for 1 h at 37°C. The enzymatic reaction was developed using *O*-phenylenediamine dihydrochloride (Sigma-Aldrich Cat # P1526) and stopped with 2 N H_2SO_4. The OD was measured at 492 nm in a microplate reader (Tecan Sunrise).

Western blot and dot blot

For western blot, 20 μg of lysate containing recombinant REST DBD was denatured in loading buffer at 98°C for 10 min (Biorad Cat # 1610747), separated by 12% sodium dodecyl sulphate polyacrylamide gel electrophoresis (SDS-PAGE) and transferred to a nitrocellulose membrane (Biorad Cat # 1620115), which was blocked with 5% skim milk in PBS-Tween 0.05% for 40 min at RT with shaking. After washing, the membrane was incubated with the mAbs at a final concentration of 10 μg/mL at RT and constant agitation, for 2 h followed by incubation with an HRP conjugated anti-mouse IgM antibody (dilution 1:2,000) in PBS-Tween 0.05%, for 1 h. Immunoreactivity was developed with 3-3′-diaminobenzidine (DAB, Sigma-Aldrich Cat # D8001). Dot blot was proven similarly using total lysate or purified recombinant REST DBD (Biorad Cat # 1620115).

Immunoprecipitation

Pure mAbs (10 μg) were incubated with 2.5 μL of protein L-agarose beads (sc-2336 Santa Cruz Biotechnology) at 4°C for 5 h, and then washed with PBS three times. Next, 100 μg of lysate containing the recombinant REST DBD, MRC5 nuclear extract or HeLa total extract with protease inhibitors, were added to the bead/antibody

complexes and incubated overnight at 4°C with constant agitation. Complexes were washed as mentioned above. Immunoprecipitated REST was monitored in 10% SDS-PAGE and Coomassie blue or silver-stained following manufacturer's instructions (Biorad Cat # 1610449).

Sample collection

We used representative cervical cytologies of normal sample (NSIL), premalignant lesions (LGSIL and HGSIL) and squamous cell carcinoma (CC), all of which were classified according to the Bethesda system (*39*). The Ethics Committee of the Autonomous University of Guerrero approved the study protocol, and each participant signed an informed consent, in accordance with the Declaration of Helsinki. Exo-endocervical exfoliated cell samples were collected by sampling the ectocervix with an Ayre spatula, and samples from the endocervix were obtained using a cytobrush to ensure that cytological material was obtained from the squamous columnar transformation zone. Cytological samples were preserved using preservative solution (liquid-PREPTM, LGM International Inc., Melbourne, FL, USA) for at least 1 h prior to processing. An aliquot (~50 μL) was placed on a clean glass microscope slide and fixed with 95% ethanol. Fixed specimens were used for immunocytochemistry (ICC).

Immunocytochemistry

The streptavidin biotin peroxidase-based immunocytochemical method was performed using the Cytoscan HRP/DAB cell detection system (Cell Marque Corporation, Hot Springs, AR, USA). The antibodies used were the mAbs and mouse hyperimmune serum produced in this study, and a commercially available H-290 antibody (Santa Cruz Biotechnology Cat # sc-25398). The cytology slides were subjected to antigen retrieval (ImmunoDNA Retriever Citrate, Bio SB, Santa Barbara, CA, USA) for 15 min at 120°C. Samples were incubated with the primary antibody (10 μg for mAbs and 1:50 commercial antibody and 1:50 hyperimmune serum) for 2 h, and then exogenous biotin and streptavidin peroxidase were added. The reaction was developed using the chromogen DAB and counterstained with Mayer's hematoxylin. In the negative control (C−), the primary antibody was omitted.

Data analysis

Analysis were performed in the GraphPad prism V.5 software and in Microsoft Excel 2016.

Results

In silico *analysis*

During mAbs production, the previous analysis of immunogenicity and antigenicity of the selected antigen plays a key role. Immunogenicity refers to the ability of the recombinant protein to induce the humoral response in the immunized mice, while the antigenicity means the ability of the recombinant protein to be recognized by the mAbs.

In search of immunogenic sites in the REST structure, we first looked for functional domains in all reported isoforms in different cancers, such as neuroblastoma, breast, lung, prostate and colorectal (*16–21*). *In silico* analysis showed that the REST gene contains three coding exons, giving rise to six mRNA variants by alternative splicing. These mRNAs codify two large proteins, one of them containing a deletion in the fifth zinc finger and four truncated isoforms (commonly named REST N-1, REST N-4, REST N50 and REST N-62). Truncated isoforms occur because of exon N insertion during alternative splicing. Notably, short isoforms contain only the N-terminal and part of the DBD, but they lack the C-terminal (Fig. 1). For immunogenicity and antigenicity analysis, the REST amino acid sequence was divided into three functional domains (N-terminal [1–152], DBD [153–466] and C-terminal [447–1,097]). Results showed that the N-terminal contains few immunogenic/antigenic sites, whereas the majority of immunogenic/antigenic sites was in the DBD and C-terminal. The DBD domain, in particular, contains the highest number of epitopes for B cell binding, as well as a large proportion of antigenic sites (Table I).

When we searched immunogenic and antigenic analogues epitopes, we found five peptides in the whole DBD structure (Fig. 2A). Since the REST DBD has not been previously crystallized, we generated the 3D structure by molecular modelling, and the RE1 sequence was coupled by docking in order to observe the location of the predicted peptides in the DBD structure and to ensure that the produced antibodies will recognize exposed peptides in the native structure. We found that all the predicted peptides are exposed and that none of them was localized in the regions that interact with DNA (Fig. 2B).

Production and preliminary characterization of anti-REST DBD monoclonal antibodies

According to our analyses, the DBD is a potential domain for the production of monoclonal antibodies against native REST. Hence, we directed mice immunization using the recombinant REST DBD, which was purified by affinity chromatography from the *E. coli* strain BL21 (DE3) harbouring the vector pET28a-REST DBD (Fig. 3A). After fusion evaluation, we obtained two clones (5G2 and 5C3) and they were subcloned twice. Finally, we obtained the G5B4, B2F9 and F2E7 final clones based on the growth and mAb *in vitro* production (Fig. 3B).

After mAbs were obtained, we determined the immunoglobulin (Ig) class, observing that all the obtained mAbs were IgM class (Fig. 4A). Bands corresponded mainly due to heavy and light chains as observed in a 12% SDS-PAGE, which was stained with Coomassie blue (Fig. 4B). In order to characterize the optimal concentrations of the mAbs and recombinant REST necessary for experiments, we performed indirect ELISA using all the clones. Results showed that sufficient mAbs signal was obtained at concentration of 10 μg/mL (Fig. 4C), whereas the measurable concentration range of recombinant REST was 1.25–20 μg/mL, without significant changes between clones (Fig. 4D).

For linear or conformational epitopes recognition, we used the recombinant DBD under denatured or native conditions in an ELISA screen, and confirmed by western blot and dot blot experiments. In ELISA, results showed that mAbs did not recognize significantly denatured REST DBD (Fig. 5A), which coincided with our western blot observations (Fig. 5B). However, we observed a robust dot blot signal when the native DBD was used (Fig. 5C). Finally, immunoprecipitation using protein L-agarose and *E. coli* total lysate transformed with pET28a-REST DBD, showed that mAb recognizes specifically recombinant DBD (Fig. 5D).

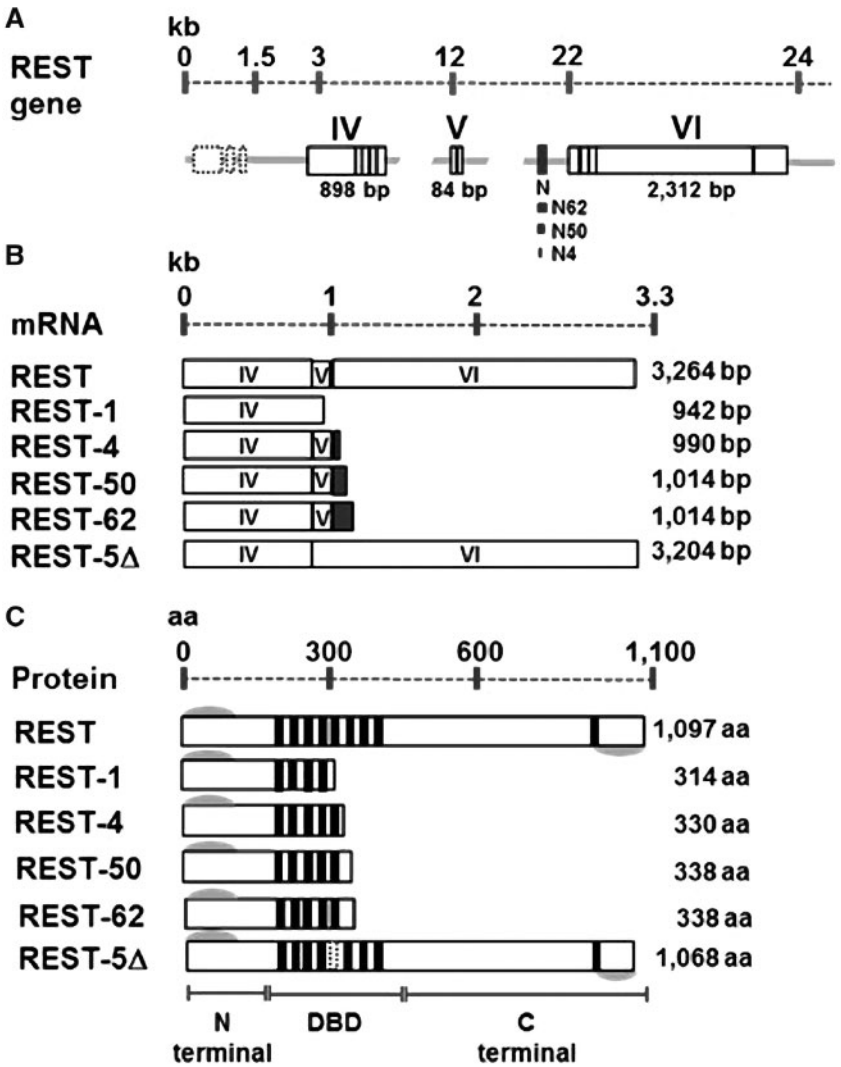

Fig. 1 Schematic representation of the REST gene, splicing variants and isoforms. (**A**) The REST gene contains three constitutive coding exons (white boxes) and one alternative exon (grey box). The size of the alternative exon N depends on 4, 50 or 62 base pair insertions (bottom black lines). (**B**) Six coding REST mRNAs are shown. The size of the translatable region depends on the number of coding exons (white boxes) and exon N insertion (grey box). (**C**) The REST protein carries three functional domains; N-terminal, DBD and C-terminal. Zinc fingers (black lines) and repressor domains (grey semi circles).

Table I. REST *in silico* analysis of immunogenic and antigenic sites

Software	Total antigenic sites *n* (%)	DBD *n* (%)	N-terminal *n* (%)	C-terminal *n* (%)
ABCpred	37 (100)	18 (48.6)	3 (8.1)	16 (43.3)
Bcepred	54 (100)	15 (27.8)	9 (16.6)	30 (55.6)
IEDB	12 (100)	4 (33.3)	3 (25)	5 (41.7)
Predicted antigenic peptides	36 (100)	15 (41.7)	3 (8.3)	18 (50)

Potential clinical use of mAb anti-REST

Epithelial tissues and cytological samples from the uterine cervix express high levels of nuclear REST with a residual cytoplasmic expression. To explore the clinical utility of mAbs and full-length protein recognition, we performed ICC assays using cervical cytology samples from women diagnosed with premalignant lesions and CC using as positive controls a commercially available antibody and mouse hyperimmune serum. When we compared our mAbs with the commercial antibody H-290 or hyperimmune serum in non-SIL and LGSIL, we observed significant expression of REST using the clone G5B4 but not with clone B2F9 or F2E7. In HGSIL and CC samples, we observed loss of nuclear REST (Fig. 6A), similar to observations made by others researchers in many types of cancer (*17–20*).

Using the clone G5B4, we also performed immunoprecipitation assays using extracts from MRC5 and

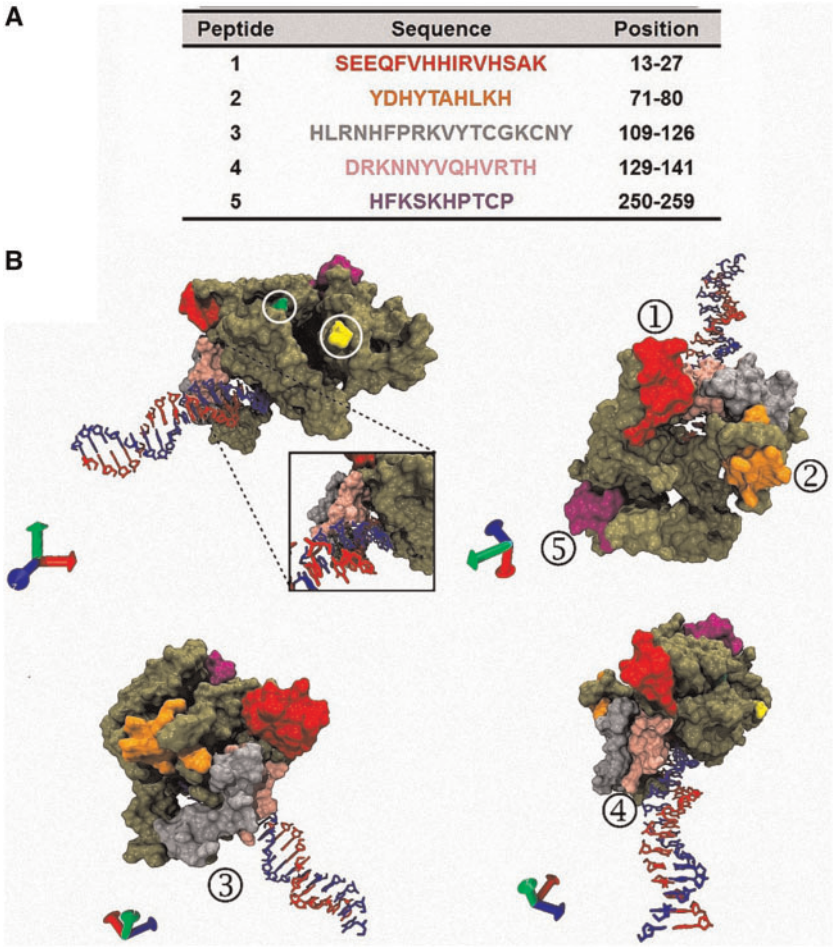

Fig. 2 Immunogenic and antigenic sites in the DBD 3D structure. (**A**) Sequence and localization of immunogenic/antigenic sites in the REST DBD amino acids sequence. (**B**) DBD 3D structure prediction and RE1 docking. Localization of predicted peptides is market with numbers. The first and last amino acids are marked with circles in the first structure.

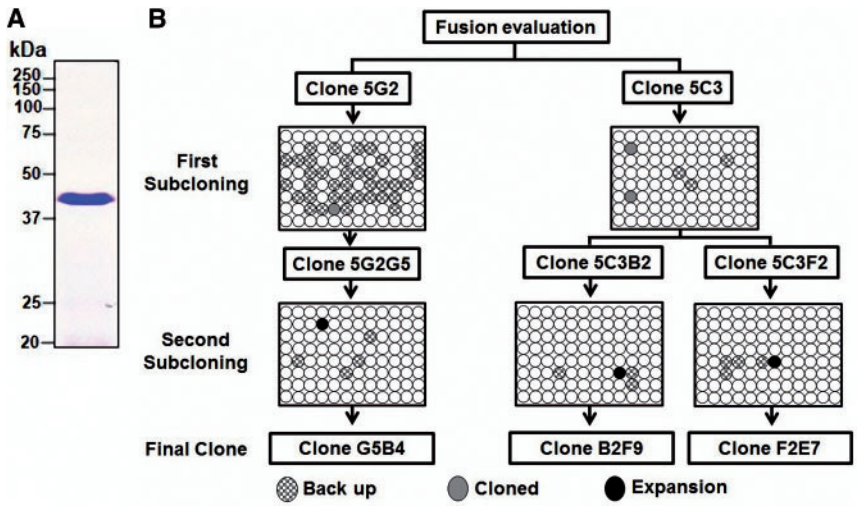

Fig. 3 Generation and selection of antibody-producing hybridomas. (**A**) Recombinant REST DBD use for immunization, monitored in 12% SDS-PAGE and stained with Coomassie blue. (**B**) mAb producing clones. Cloning and subcloning were performed by limiting dilution.

HeLa cell lines. A complete large isoform and truncated isoforms were observed in MRC5 and HeLa, respectively, indicating the ability of this antibody to recognize native forms of REST (Fig. 6B).

Discussion

Current evidences shows the role of REST in the neural lineages definition during neurogenesis, neural

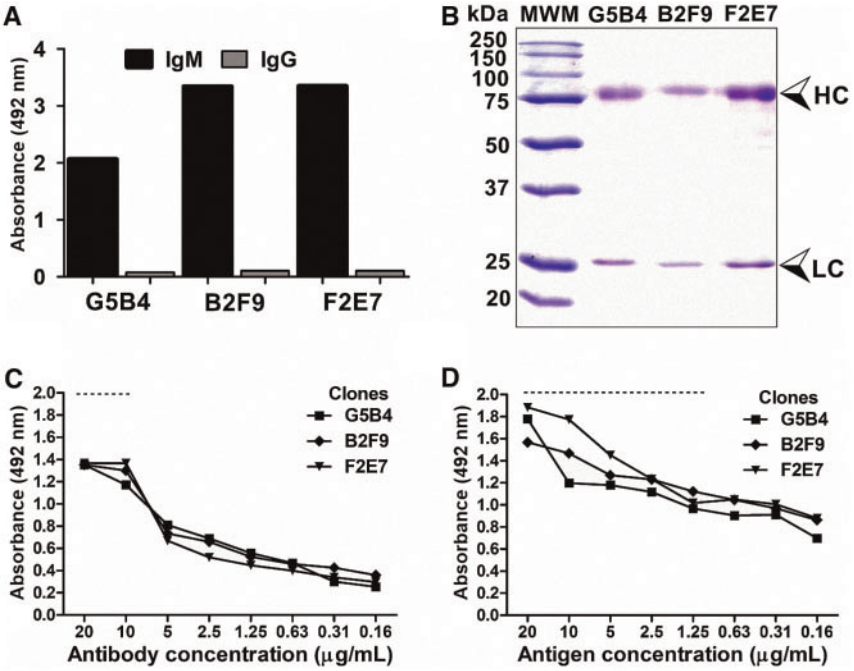

Fig. 4 Primary characterization of mAbs. (**A**) Ig class determination. Secondary antibodies against the heavy μ (IgM) and γ (IgG) chains conjugated to HRP were used. (**B**) Purity evaluation of the obtained mAbs by SDS-PAGE and Coomassie blue staining. HC, heavy chain; LC, light chain. (**C**) Antibody titration and (**D**) antigen concentration recognized by each clone, mAbs were used as the primary antibody and an anti-mouse IgM HRP conjugated was used as a secondary antibody. Absorbance was determined at 492 nm.

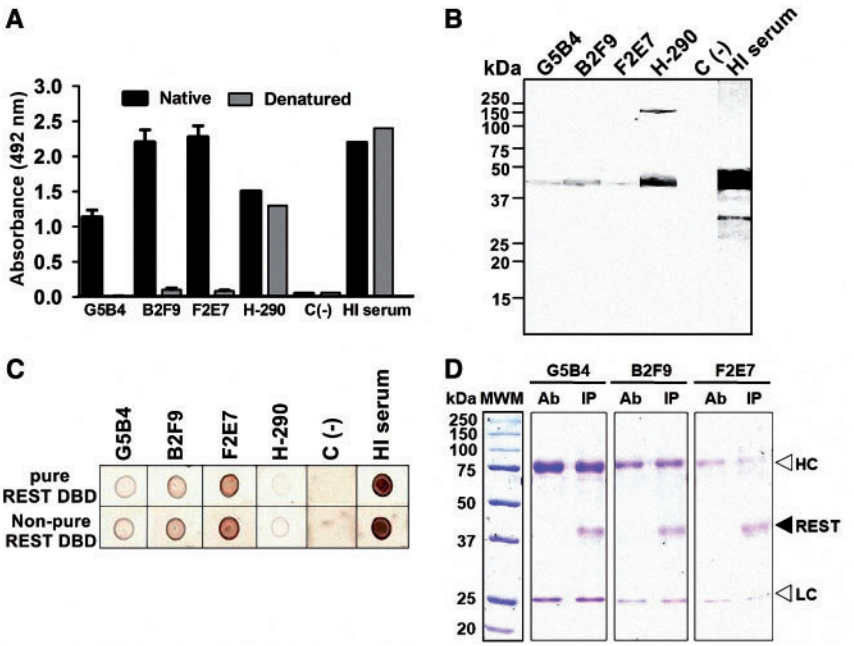

Fig. 5 Preliminary characterization of the produced mAbs. (**A**) Indirect ELISA using native and denatured REST DBD purified protein (absorbance was determined at 492 nm). (**B**) Western blot and (**C**) dot blot using as antigen *E. coli* BL21 (DE3) total lysate transformed with the construction pET28a-REST DBD and purified protein (dot blot) at a final concentration of 20 μg/mL. Primary antibody: obtained mAbs, commercial antibody H-290 (Santa Cruz biotechnology Cat # sc-25398) or mouse hyperimmune serum. Secondary antibody: HRP-conjugated anti-mouse IgM or anti-rabbit IgG conjugated to HRP. (**D**) Immunoprecipitation using protein L-agarose. Ab: antibody/beads complex and IP: antibody/beads/antigen complex. The antigen used was total lysate of *E. coli* BL21 (DE3) transformed with pET28a-REST DBD. Arrows indicate HC (heavy chain), LC (light chain) and recombinant REST.

plasticity, neuronal and non-neuronal fate maintenance in adults, motility, angiogenesis and cell cycle regulation (*9*, *40*, *41*). In addition, the role of REST in cancer is well demonstrated in cell lines and patients' samples, where a variety of short isoforms of REST is present (*18*, *19*, *23*), supporting the idea of the use of REST as a biomarker. For this reason, commercial antibodies have been designed for C-terminal of

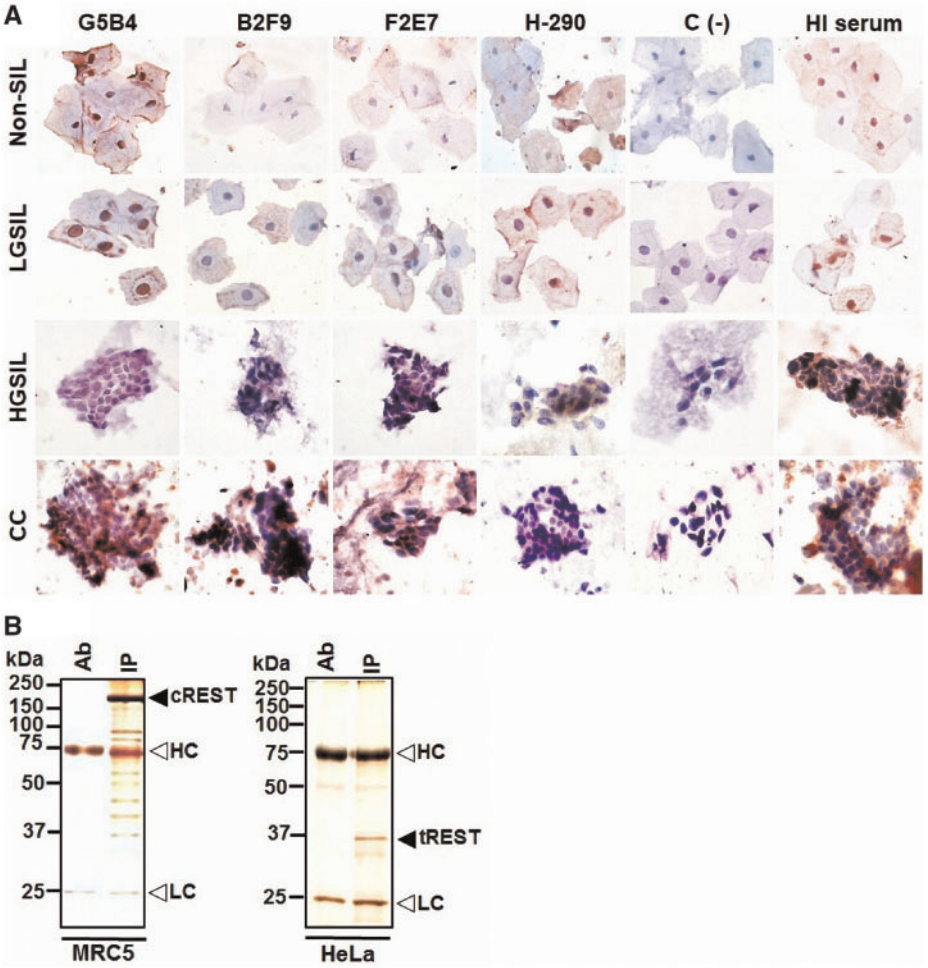

Fig. 6 mAbs recognition to full-length REST from cells. (**A**) ICC using anti-REST mAbs and cytology samples derived from women diagnosed with of premalignant lesions and CC. Non-SIL, non-squamous intraepithelial lesion; LGSIL, low grade-squamous intraepithelial lesion; HGSIL, high grade-squamous intraepithelial lesion; CC, cervical cancer; HI serum, hyperimmune serum; and C (−), negative control. (**B**) Immunoprecipitation using protein L-agarose beads. Left panel: MRC5 cells, and right panel: HeLa cells. Arrows indicate HC, heavy chain; LC, light chain; cREST, canonic REST and tREST, truncated REST.

REST recognition, which is lost during carcinogenesis (*17*). Nevertheless, the clinical use of these antibodies has not been approved. In this work, we designed a strategy for the production of specific antibodies capable of recognizing REST in samples from patients.

In silico data showed the presence of five immunogenic sites in the DBD and three sites in the C-terminal. The DBD is conserved across mammals (*8*) and the observed immunogenic sites correspond to zinc finger motifs or spacer sequences ranging from 9 to 17 amino acids. Interestingly, at least two immunogenic sites are present in all short REST isoforms, which could be relevant target for mAbs design. Notably, the relevant peptides identified in the DBD presented hydrophilicity, antigenicity and good interaction with major histocompatibility complex (MHC) molecules, which are necessary characteristics for immunogenicity (*42*).

The presence of DBD in almost all REST isoforms and the absence of the C-terminal in short isoforms in a range of cancers is relevant because these regions constitutes differential targets in the antibody design. However, many of commercial antibodies are designed to target the C-terminal and they are not suitable for detecting truncated REST isoforms in cancer generated by the insertion of the alternative exon N (*17*, *43*). Examples of this argument can be reviewed in the Antibodypedia database (https://www.antibodypedia.com), where mAbs against the C-terminal have been previously produced for research purposes but not for diagnosis.

An important part of the characterization process of a monoclonal antibody is the dissection of the epitope type that is recognized, which can help to determine the possible usefulness of the generated mAb (*44*). The mAbs produced in this work recognized both the native recombinant and complete structure of REST at concentrations ranging 1 to 20 μg/mL, but not denatured epitopes, suggesting that they could identify conformational proteins. Actually, the use of these antibodies could be limited to techniques requiring native protein, such as ELISA, dot blot, immunoprecipitation and ICC, as we showed herein. In this work, we performed the ICC method, a non-invasive variant of immunohistochemistry commonly used for the diagnosis prediction, prognosis and clinical management of

patients with cancer (*45*). A concise nuclear expression in normal samples and loss of nuclear expression and cytoplasmic accumulation of REST in HGSIL and CC samples were observed with the clone G5B4, hyperimmune serum and commercial antibody, which is in accordance with previous observations made by our workgroup and others (*46*, *47*). In addition, we observed the full-length REST in the non-cancerous cell line MRC5 and a truncated isoform in HeLa cells (adenocarcinoma derived cell line) by means immunoprecipitation experiments.

Previously it has been reported that the expression of short isoforms lacking the C-terminal and the loss of the canonic REST is associated with the prognosis and tumourigenicity of cancer (*19–21*), as well as increased proliferation, decreased apoptosis (*18*, *48*) and neuronal genes activation, which all together impact in the oncogenic properties and cellular phenotype transformation of cancer cells (*22*, *23*). Considering these arguments, the mAbs against REST described here could be used for standardization of a sensitive and specific immunoassay to evaluate the use of REST as a biomarker in the different types of cancer and in neuropathies in which its expression is altered. However, it is necessary to perform further assays for antibody validation using adequate positive and negative controls, in accordance with the guidelines proposed by the International Working Group for Antibody Validation (*49*).

Finally, this work provides evidence about the design, production and characterization of clones producing mAbs against the REST DBD. It constitutes an achievement in the field of cancer biomarkers, and an opportunity to explore the role of REST during carcinogenesis, although it is necessary to corroborate the potential use in clinical diagnostics by evaluating REST expression in a significant number of clinical samples from different types of cancer.

Acknowledgements

During this work, Karen Cortés Sarabia was awarded with a doctorate scholarship by CONACYT (National Council of Science and Technology) with registration number 557803. We are very grateful to Adán Arizmendi Izazaga and Hector Javier Lasso Avila for technical support in Fig. 1 and to Elder Ortuño for manuscript review and comments.

Funding

The Autonomous University of Guerrero supported this work, grant Programa Fortalecimiento de la Calidad Educativa 2017 (UAGRO-CA-109).

Conflict of Interest

None declared.

References

1. Schoenherr, C.J. and Anderson, D.J. (1995) The neuron-restrictive silencer factor (NRSF): a coordinate repressor of multiple neuron-specific genes. *Science* **267**, 1360–1363
2. Bruce, A.W., Donaldson, I.J., Wood, I.C., Yerbury, S.A., Sadowski, M.I., Chapman, M., Göttgens, B., and Buckley, N.J. (2004) Genome-wide analysis of repressor element 1 silencing transcription factor/neuron-restrictive silencing factor (REST/NRSF) target genes. *Proc. Natl. Acad. Sci. USA* **01**, 10458–10463
3. Jones, F.S. and Meech, R. (1999) Knockout of REST/NRSF shows that the protein is a potent repressor of neuronally expressed genes in non-neural tissues. *Bioessays* **21**, 372–376
4. Mulligan, P., Westbrook, T.F., Ottinger, M., Pavlova, N., Chang, B., Macia, E., Shi, Y.-J., Barretina, J., Liu, J., Howley, P.M., Elledge, S.J., and Shi, Y. (2008) CDYL bridges REST and histone methyltransferases for gene repression and suppression of cellular transformation. *Mol. Cell* **32**, 718–726
5. Saritas-Yildirim, B., Childers, C.P., Elsik, C.G., and Silva, E.M. (2015) Identification of REST targets in the *Xenopus tropicalis* genome. *BMC Genomics* **16**, 380
6. Schoenherr, C., Paquette, A.J., and Anderson, D.J. (1996) Identification of potential target genes for the neuron-restrictive silencer factor. *Proc. Natl. Acad. Sci. USA* **93**, 9881–9886
7. Faronato, M. and Coulson, J. (2011) REST (RE1-silencing transcription factor). *Atlas Genet. Cytogenet. Oncol. Haematol* **15**, 208–213
8. Palm, K., Belluardo, N., Metsis, M., and Timmusk, T. (1998) Neuronal expression of zinc finger transcription factor REST/NRSF/XBR gene. *J. Neurosci.* **18**, 1280–1296
9. Nechiporuk, T., McGann, J., Mullendorff, K., Hsieh, J., Wurst, W., Floss, T., and Mandel, G. (2016) The REST remodeling complex protects genomic integrity during embryonic neurogenesis. *eLife* **5**, 09584
10. Sun, Y.-M., Greenway, D.J., Johnson, R., Street, M., Belyaev, N.D., Deuchars, J., Bee, T., Wilde, S., and Buckley, N.J. (2005) Distinct profiles of REST interactions with its target genes at different stages of neuronal development. *Mol. Biol. Cell* **16**, 5630–5638
11. Canzonetta, C., Mulligan, C., Deutsch, S., Ruf, S., O'Doherty, A., Lyle, R., Borel, C., Lin-Marq, N., Delom, F., Groet, J., Schnappauf, F., De Vita, S., Averill, S., Priestley, J.V., Martin, J.E., Shipley, J., Denyer, G., Epstein, C.J., Fillat, C., Estivill, X., Tybulewicz, V.L.J., Fisher, E.M.C., Antonarakis, S.E., and Nizetic, D. (2008) DYRK1A-dosage imbalance perturbs NRSF/REST levels, deregulating pluripotency and embryonic stem cell fate in Down syndrome. *Am. J. Hum. Genet.* **83**, 388–400
12. Majumder, S. (2006) REST in good times and bad: roles in tumor suppressor and oncogenic activities. *Cell Cycle* **5**, 1929–1935
13. Schiffer, D., Caldera, V., Mellai, M., Conforti, P., Cattaneo, E., and Zuccato, C. (2014) Repressor element-1 silencing transcription factor (REST) is present in human control and Huntington's disease neurons. *Neuropathol. Appl. Neurobiol.* **40**, 899–910
14. Huang, Z. and Bao, S. (2012) Ubiquitination and deubiquitination of REST and its roles in cancers. *FEBS Lett.* **586**, 1602–1605
15. Walker, G.E., Antoniono, R.J., Ross, H.J., Paisley, T.E., and Oh, Y. (2006) Neuroendocrine-like differentiation of non-small cell lung carcinoma cells: regulation by cAMP and the interaction of mac25/IGFBP-rP1 and 25.1. *Oncogene* **25**, 1943–1954
16. Westbrook, T.F., Martin, E.S., Schlabach, M.R., Leng, Y., Liang, A.C., Feng, B., Zhao, J.J., Roberts, T.M.,

Mandel, G., Hannon, G.J., Depinho, R.A., Chin, L., and Elledge, S.J. (2005) A genetic screen for candidate tumor suppressors identifies REST. *Cell* **121**, 837–848

17. Coulson, J.M., Edgson, J.L., Woll, P.J., and Quinn, J.P. (2000) A splice variant of the neuron-restrictive silencer factor repressor is expressed in small cell lung cancer: a potential role in derepression of neuroendocrine genes and a useful clinical marker. *Cancer Res.* **60**, 1840–1844
18. Lv, H., Pan, G., Zheng, G., Wu, X., Ren, H., Liu, Y., and Wen, J. (2010) Expression and functions of the repressor element 1 (RE-1)-silencing transcription factor (REST) in breast cancer. *J. Cell. Biochem.* **110**, 968–974
19. Reddy, B.Y., Greco, S.J., Patel, P.S., Trzaska, K.A., and Rameshwar, P. (2009) RE-1-silencing transcription factor shows tumor-suppressor functions and negatively regulates the oncogenic TAC1 in breast cancer cells. *Proc. Natl. Acad. Sci. USA* **106**, 4408–4413
20. Wagoner, M.P., Gunsalus, K.T.W., Schoenike, B., Richardson, A.L., Friedl, A., and Roopra, A. (2010) The transcription factor REST is lost in aggressive breast cancer. *PLoS Genet.* **6**, e1000979
21. Svensson, C., Ceder, J., Iglesias-Gato, D., Chuan, Y.-C., Pang, S.T., Bjartell, A., Martinez, R.M., Bott, L., Helczynski, L., Ulmert, D., Wang, Y., Niu, Y., Collins, C., and Flores-Morales, A. (2014) REST mediates androgen receptor actions on gene repression and predicts early recurrence of prostate cancer. *Nucleic Acids Res.* **42**, 999–1015
22. Fuller, G.N., Su, X., Price, R.E., Cohen, Z.R., Lang, F.F., Sawaya, R., and Majumder, S. (2005) Many human medulloblastoma tumors overexpress repressor element-1 silencing transcription (REST)/neuron-restrictive silencer factor, which can be functionally countered by REST-VP16. *Mol. Cancer Ther.* **4**, 343–349
23. Kamal, M.M., Sathyan, P., Singh, S.K., Zinn, P.O., Marisetty, A.L., Liang, S., Gumin, J., El-Mesallamy, H.O., Suki, D., Colman, H., Fuller, G.N., Lang, F.F., and Majumder, S. (2012) REST regulates oncogenic properties of glioblastoma stem cells. *Stem Cells* **30**, 405–414
24. Yu, Y., Li, S., Zhang, H., Zhang, X., Guo, D., and Zhang, J. (2018) NRSF/REST levels are decreased in cholangiocellular carcinoma but not hepatocellular carcinoma compared with normal liver tissues: a tissue microarray study. *Oncol. Lett.* **15**, 6592–6598
25. Varghese, B.V., Koohestani, F., McWilliams, M., Colvin, A., Gunewardena, S., Kinsey, W.H., Nowak, R.A., Nothnick, W.B., and Chennathukuzhi, V.M. (2013) Loss of the repressor REST in uterine fibroids promotes aberrant G protein-coupled receptor 10 expression and activates mammalian target of rapamycin pathway. *Proc. Natl. Acad. Sci. USA* **110**, 2187–2192
26. Chen, G.-L. and Miller, G.M. (2013) Extensive alternative splicing of the repressor element silencing transcription factor linked to cancer. *PLoS One* **8**, e62217
27. Saha, S. and Raghava, G. (2006) Prediction of continuous B-cell epitopes in an antigen using recurrent neural network. *Proteins* **65**, 40–48
28. Saha, S., Raghava, G.P.S. (2004) BcePred: Prediction of Continuous B-Cell Epitopes in Antigenic Sequences Using Physico-chemical Properties. *ICARIS, Lect Notes Comput Sci* **3239**, 197–204
29. Kolaskar, A.S. and Tongaonkar, P.C. (1990) A semi-empirical method for prediction of antigenic determinants on protein antigens. *FEBS Lett.* **276**, 172–174
30. Vita, R., Overton, J.A., Greenbaum, J.A., Ponomarenko, J., Clark, J.D., Cantrell, J.R., Wheeler, D.K., Gabbard, J.L., Hix, D., Sette, A., and Peters, B. (2015) The immune epitope database (IEDB) 3.0. *Nucleic Acids Res.* **43**, D405–D412
31. Roy, A., Kucukural, A., and Zhang, Y. (2010) I-TASSER: a unified platform for automated protein structure and function prediction. *Nat. Protoc.* **5**, 725–738
32. Yang, J., Yan, R., Roy, A., Xu, D., Poisson, J., and Zhang, Y. (2015) The I-TASSER suite: protein structure and function prediction. *Nat. Methods* **12**, 7–8
33. Zhang, Y. (2008) I-TASSER server for protein 3D structure prediction. *BMC Bioinformatics* **9**, 40
34. Colovos, C. and Yeates, T.O. (1993) Verification of protein structures: patterns of nonbonded atomic interactions. *Protein Sci.* **2**, 1511–1519
35. Lu, X.-J. and Olson, W.K. (2003) 3DNA: a software package for the analysis, rebuilding and visualization of three-dimensional nucleic acid structures. *Nucleic Acids Res.* **31**, 5108–5121
36. van Dijk, M. and Bonvin, A. (2009) 3D-DART: a DNA structure modelling server. *Nucleic Acids Res.* **37**, W235–W239
37. Tuszynska, I., Magnus, M., Jonak, K., Dawson, W., and Bujnicki, J.M. (2015) NPDock: a web server for protein-nucleic acid docking. *Nucleic Acids Res.* **43**, W425–W430
38. Köhler, G. and Milstein, C. (1975) Continuous cultures of fused cells secreting antibody of predefined specificity. *Nature* **256**, 495–497
39. Nayar, R. and Wilbur, D.C. (2015) The pap test and Bethesda 2014. *Acta Cytol.* **59**, 121–132
40. Lunyak, V.V. and Rosenfeld, M.G. (2005) No rest for REST: rEST/NRSF regulation of neurogenesis. *Cell* **121**, 499–501
41. Magistrelli, G. and Malinge, P. (2014) Antigen Production for Monoclonal Antibody Generation. (Ossipow V. and Fischer N., eds.) pp. 3–20, Humana Press, Totowa, NJ
42. Johnson, R., Samuel, J., Ng, C.K.L., Jauch, R., Stanton, L.W., and Wood, I.C. (2009) Evolution of the vertebrate gene regulatory network controlled by the transcriptional repressor REST. *Mol. Biol. Evol.* **26**, 1491–1507
43. Ortuño-Pineda, C., Galindo-Rosales, J.M., Calderón-Salinas, J.V., Villegas-Sepúlveda, N., Saucedo-Cárdenas, O., De Nova-Ocampo, M., and Valdés, J. (2012) Binding of hnRNP H and U2AF65 to respective G-codes and a poly-uridine tract collaborate in the N50-5'ss selection of the REST N Exon in H69 Cells. *PLoS One* **7**, e40315
44. Forsström, B., Bisławska Axnäs, B., Rockberg, J., Danielsson, H., Bohlin, A., and Uhlen, M. (2015) Dissecting antibodies with regards to linear and conformational epitopes. *PLoS One* **10**, e0121673
45. Bordeaux, J., Welsh, A., Agarwal, S., Killiam, E., Baquero, M., Hanna, J., Anagnostou, V., and Rimm, D. (2010) Antibody validation. *BioTechniques* **48**, 197–209
46. Shimojo, M. (2006) Characterization of the nuclear targeting signal of REST/NRSF. *Neurosci. Lett.* **398**, 161–166
47. Westbrook, T.F., Hu, G., Ang, X.L., Mulligan, P., Pavlova, N.N., Liang, A., Leng, Y., Maehr, R., Shi, Y., Harper, J.W., and Elledge, S.J. (2008) SCFbeta-TRCP controls oncogenic transformation and neural differentiation through REST degradation. *Nature* **452**, 370–374

48. Baiula, M., Carbonari, G., Dattoli, S.D., Calienni, M., Bedini, A., and Spampinato, S. (2012) REST is up-regulated by epidermal growth factor in HeLa cells and inhibits apoptosis by influencing histone H3 acetylation. *Biochim. Biophys. Acta* **1823**, 1252–1263

49. Uhlen, M., Bandrowski, A., Carr, S., Edwards, A., Ellenberg, J., Lundberg, E., Rimm, D.L., Rodriguez, H., Hiltke, T., Snyder, M., and Yamamoto, T. (2016) A proposal for validation of antibodies. *Nat. Methods* **13**, 823–827